Biochimica et Biophysica Acta 1798 (2010) 938–946

Contents lists available at ScienceDirect

Biochimica et Biophysica Acta

journal homepage: www.elsevier.com/locate/bbamem

Membrane simulations mimicking acidic pH reveal increased thickness and negative curvature in a bilayer consisting of lysophosphatidylcholines and free fatty acids

Katariina Lähdesmäki [a,*], O.H. Samuli Ollila [b], Artturi Koivuniemi [b], Petri T. Kovanen [a], Marja T. Hyvönen [a,c]

[a] Wihuri Research Institute, Kalliolinnantie 4, FIN-00140 Helsinki, Finland
[b] Department of Physics, Tampere University of Technology, P.O. Box 692, FIN-33101 Tampere, Finland
[c] Department of Physical Sciences, Biophysics, P.O. Box 3000, FIN-90014 University of Oulu, Finland

ARTICLE INFO

Article history:
Received 11 September 2009
Received in revised form 18 December 2009
Accepted 22 January 2010
Available online 2 February 2010

Keywords:
MD-simulation
Phospholipid
pH
Phospholipase A_2
Lateral pressure profile
Spontaneous curvature

ABSTRACT

Phospholipids are key components of biological membranes and their lipolysis with phospholipase A_2 (PLA_2) enzymes occurs in different cellular pH environments. Since no studies are available on the effect of pH on PLA_2-modified phospholipid membranes, we performed 50-ns atomistic molecular dynamics simulations at three different pH conditions (pH 9.0, 7.5, and 5.5) using a fully PLA_2-hydrolyzed phosphatidylcholine (PC) bilayer which consists solely of lysophosphatidylcholine and free fatty acid molecules. We found that a decrease in pH results in lateral squeezing of the membrane, i.e. in decreased surface area per headgroup. Thus, at the decreased pH, the lipid hydrocarbon chains had larger S_{CD} order parameter values, and also enhanced membrane thickness, as seen in the electron density profiles across the membrane. From the lateral pressure profiles, we found that the values of spontaneous curvature of the two opposing monolayers became negative when the pH was decreased. At low pH, protonation of the free fatty acid headgroups reduces their mutual repulsion and accounts for the pH dependence of all the above-mentioned properties. The altered structural characteristics may significantly affect the overall surface properties of biomembranes in cellular vesicles, lipid droplets, and plasma lipoproteins, play an important role in membrane fission and fusion, and modify interactions between membrane lipids and the proteins embedded within them.

1. Introduction

Biological membranes are mainly composed of phospholipids, assembled into either bilayers or monolayers [1]. A growing interest lies in understanding the biophysical properties of membranes that directly affect cellular fission and fusion events [2], and the functions of various proteins in cellular membranes [3].

Membrane fission and fusion are mechanistically related events, both of which involve strong membrane bending and highly curved non-bilayer lipid intermediates [2,4,5]. In the formation of such highly curved lipid intermediates, phospholipids and lysophospholipids are proposed to play key roles [6,7]. The process of membrane bending depends on spontaneous curvature, which is influenced by external factors such as pH, temperature, and salt concentration. Indeed, in experiments with phosphatidic acid membranes, low pH together with divalent cations was found to promote negative spontaneous curvature and the conversion to a hexagonal H_{II} phase [7–9]. Both low pH and divalent cations can induce headgroup dehydration, and thus reduce the effective headgroup size, by neutralizing the negatively charged headgroup regions. Increasing evidence proposes that intermediate structures having negative monolayer curvature are involved in membrane fusion [4], an event that requires the interplay between membrane lipids and proteins [10,11]. In experimental studies of complex model systems, fusion appears to be partly determined by the properties of lipids [12]; corroborating evidence was also found from extensive atomistic simulations [13].

In addition to the external factors, among them pH, bending of the membrane may also require changes in atomic charges and molecular shapes of the membrane lipids [7]. *In vivo*, lipid shapes are altered by lipolytic enzymes, such as the phospholipase A_2 (PLA_2) enzymes. This family of enzymes includes secretory, cytosolic, calcium-independent, and lysosomal forms, as well as the platelet-activating factor acetylhydrolase (PAF-AH) [14,15]; all hydrolyze the *sn*-2 fatty acyl ester bond of phospholipids, leading to the release of lysophosphatidylcholines (lysoPCs) and free fatty acids (FFAs) (see Fig. 1). PLA_2 has been proposed to generate high levels of hydrolysis products at highly localized regions of membranes and thus to directly affect membrane curvature [16]. The enzymatic action of PLA_2 in local membrane areas can be understood by the observation that many PLA_2 enzymes have been shown to hydrolyze their substrates in a "scooting" mode, *i.e.* to remain tightly bound to a membrane and catalyze the hydrolysis of even hundreds of phospholipids without leaving the membrane [17]. Such prolonged local hydrolytic action of the enzyme may create fully hydrolyzed nanodomains in the affected

* Corresponding author. Tel.: +358 9 681 411; fax: +358 9 637 476.
E-mail address: katariina.lahdesmaki@wri.fi (K. Lähdesmäki).

0005-2736/$ – see front matter © 2010 Elsevier B.V. All rights reserved.
doi:10.1016/j.bbamem.2010.01.020

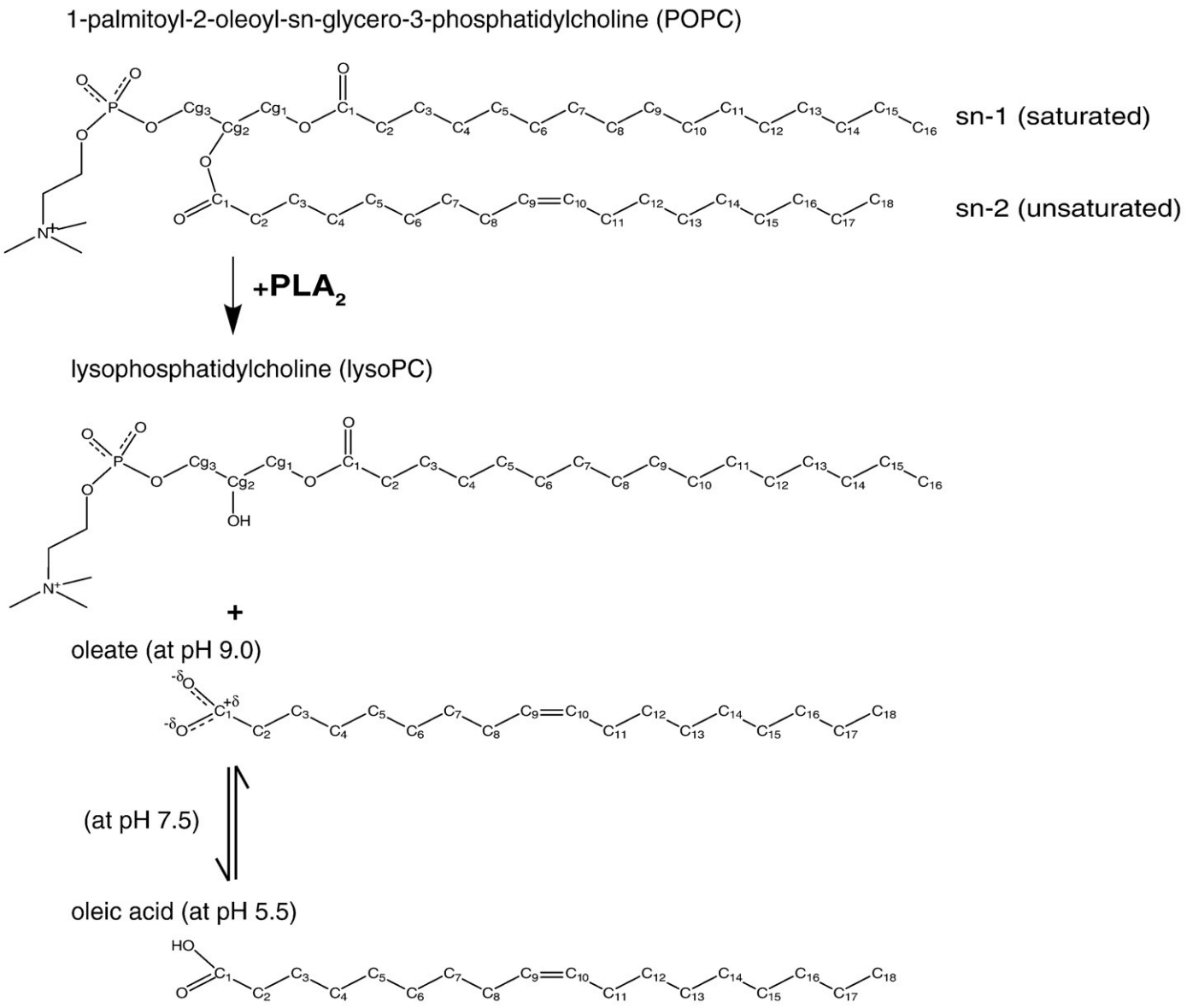

Fig. 1. Schematic molecular structures of the molecules used in the simulations: 1-palmitoyl-2-oleoyl-*sn*-glycero-3-phosphatidylcholine (POPC), in which palmitic acid is in the *sn*-1 position and oleic acid in the *sn*-2 position; POPC is PLA_2-hydrolyzed, yielding its lipolysis products lysophosphatidylcholine (lysoPC) and free fatty acid (FFA). The released FFA is at pH 9.0 in charged form (oleate), at pH 5.5 in uncharged form (oleic acid), and at pH 7.5 in both oleate and oleic acid forms. Due to pKa values of the lysoPC its protonation state doesn't change at pH 9.0–5.5.

membranes. Indeed, in the present work extremely small surface membrane area consisting of 64 POPC molecules is intended to reflect such a physiological nanodomain. Importantly, the lipolytic products generated by the PLA_2 activity contribute to membrane tubulation from the Golgi [16,18], to synaptic vesicle release [19], and to the formation of lipid droplets from the endoplasmic reticulum [20]. In addition, the cytosolic lipid droplets can increase their size by fusion [21]. In this context it is of interest that cytosolic PLA_2 enzymes can be associated to cytosolic lipid droplets and can be translocated to their surface in response to some of the lipolytic products generated by this enzyme [22,23].

Importantly, the PLA_2-catalyzed hydrolysis reaction can also proceed in an acidic environment [24,25], so allowing it to be active in the Golgi complex and the lysosome, two cellular compartments, in which the phospholipid membranes are exposed to acidic pH. In addition, the extracellular low density lipoprotein particles of the atherosclerotic arterial intima are exposed to acidic pH conditions [26] and to extensive PLA_2 hydrolysis, which then provokes their aggregation and fusion, two phenomena considered to be atherogenic [27,28]. Thus, there is ample evidence that membrane phospholipids are exposed to low pH conditions and that local regions of the membrane can be extensively lipolyzed by PLA_2 enzymes, both intracellularly and extracellularly.

In the present work, we have simulated a fully hydrolyzed 1-palmitoyl-2-oleoyl-*sn*-glycero-3-phosphocholine (POPC) bilayer at three different pH values, and compared the properties of these three systems to an unhydrolyzed POPC bilayer, which is resistent to pH-induced changes within pH values ranging from 9.0 to 5.5. Based on our results, at low pH the lipolyzed bilayer becomes more tightly packed laterally, and, moreover, differences in lateral pressure profiles indicate that spontaneous curvature values of opposing monolayer leaflets become more negative. Finally, the results suggest that the surface tension and the spontaneous curvature of a phospholipid surface monolayer on a PLA_2-modified lipoprotein particle depends on pH, which would render the tendency of lipoprotein particles to fuse pH dependent.

2. Materials and methods

2.1. Simulation details

Molecular dynamics (MD) simulations were run using the GROMACS 3.2.1 simulation package [29,30]. We simulated three lipid bilayer systems, each comprised of 128 1-palmitoyl-2-hydroxy-*sn*-glycero-3-phosphocholine (lysoPC), and 128 free fatty acid molecules (FFA) in the form of uncharged oleic acid or charged oleate (see sketches in Fig. 1). Since we are mainly interested in the effects of pH on lipolyzed phospholipid bilayers, we vary the number of oleate and oleic acid molecules in the simulated bilayers (Table 1).

Initially, the force-field parameters were adapted from a previously validated description of a pure fully hydrated dipalmitoylphosphatidylcholine bilayer (DPPC) [31], the bonded and nonbonded interactions of which are from molecular dynamics simulation study of a pure DPPC bilayer [32]. Partial charges are from ab initio calculations [33]. Explicit hydrogens are used for the hydroxyl groups of both lysoPC and oleic acid molecules. The bonded and nonbonded parameters for these hydroxyl groups are from the GROMOS force field [34], and the partial charges are from standard GROMACS building blocks [29]. The C = C double bond parameters are from the GROMOS force field and are similar to those used in previously published simulation studies concerning POPC [35,36].

As a starting structure, we used the coordinates of a fully hydrated POPC bilayer from our earlier 50 ns POPC simulation [36]. The hydrolysis of the *sn*-2 fatty acid bond was executed on the starting structure, resulting in the formation of lysoPC molecules, and oleic acid or oleate molecules. The bilayer was aligned to have the normal parallel to the *z* axis. The studied molecules together with POPC are introduced in Fig. 1. In the simulated bilayer systems we mimic three different pH conditions (pH 9, pH 7.5, and pH 5.5) by varying the amounts of oleic acid and oleate according to Table 1. Oleic acid has an experimental pKa value of 7.5 when incorporated into a lipid bilayer [37]. Thus, at high pH the fatty acid chain appears in its negatively charged oleate form and at low pH in its uncharged oleic acid form. At pH 7.5 both charged oleate and uncharged oleic acid molecules appear in equivalent amounts. Each starting structure was stabilized by energy minimization. All three systems were hydrated with 3682 water molecules. In systems with negatively charged oleate chains, 128 or 64 water molecules were randomly chosen and replaced by Na^+ ions, in order to have an overall uncharged system. Finally, the energies of the whole systems were minimized again.

The time step in the MD simulations was 2.0 fs. The bonds of the lipid molecules were constrained by the LINCS algorithm [38] and of the water molecules by using SETTLE [39]. Lennard–Jones interactions were cut off at 1.0 nm. Long-range electrostatic interactions were handled using the particle-mesh Ewald (PME) method [40], with a real-space cut-off of 1.0 nm, which has been shown to give reasonable results to account for long-range interactions in lipid bilayer systems [41], especially when charged molecules are present [42]. The simulations were performed in the NpT ensemble at 1 bar and $T = 310$ K. In the beginning, the systems were simulated for 8.0 ns using the Berendsen thermostat and barostat [43]. After this equilibration time, we switched to the Nosé–Hoover temperature coupling [44,45] and Parrinello–Rahman pressure coupling [46,47]. The coupling constant for pressure was $\tau_p = 1.0$ ps, and for temperature $\tau_t = 0.1$ ps. In total, the systems were simulated for 50 ns, of which 20 ns was regarded as an equilibration period and was not included in the analysis described below.

Table 1
Number of molecules in the three simulated systems mimicking compositions at pH 9.0, 7.5, and 5.5. Due to the pK_a value of 7.5, the fatty acid is charged at pH 9.0 and uncharged at pH 5.5. At pH 7.5 the FFA appears as an uncharged and as a charged molecule in equal amounts. The charges of the systems were neutralized by replacing some water molecules with Na^+ ions.

pH	lysoPC	FFA	Negatively charged FFA	Na^+
9.0	128		128	128
7.5	128	64	64	64
5.5	128	128		

2.2. Pressure profile calculations

The lateral pressure calculation was performed using the same procedure as explained in detail in our previous work [36] and applied to our earlier publications [36,48–50]. The previous results obtained with this approach are in good agreement with results obtained by other methods [51]. Here we introduce only the most essential features of the method used for lateral pressure calculations. First, we divide the system into approximately 0.1 nm thick slabs and calculate the local pressure tensor in each slab using the Irving–Kirkwood definition [52]. The local pressure calculation was made as post-trajectory analysis, i.e., positions and velocities saved during the simulation were used to calculate the virial at each time step, and, from these, the average over time was taken. We used PME in the actual simulations, but a cut-off of 2 nm in the pressure calculation, because there are no pairwise forces in PME. Using cut-off distance in pressure calculation causes systematic error in the results. However, as our aim is to compare differences between simulated systems, we may assume that the systematic error is not significant, since it is present in all our systems. Pressure calculation results were also confirmed with a 2.5 nm cut-off distance.

3. Results and discussion

3.1. Area per headgroup

One of the most important characteristics of a lipid bilayer is the average area per lipid molecule. Here we calculate the equilibrium area per headgroup by dividing the area of the simulation box by the number of the headgroups in a monolayer. This property can be directly compared to the area per molecule in a POPC bilayer or monolayer. This would not be the case for the area per molecule, because the lipolysis of one POPC yields two molecules: a lysoPC and a FFA. Therefore, one should also keep in mind that the area per headgroup consists of both lysoPC and FFA, but is not necessarily equally divided between them. We found the average area per headgroup for lipolysis products, to be 0.81 ± 0.02 nm^2 at pH 9, $0.66 \pm$

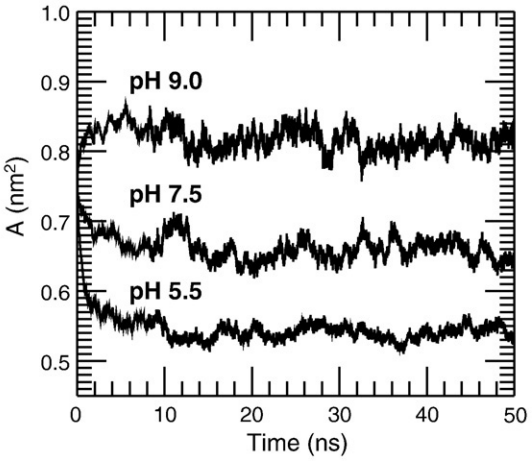

Fig. 2. Area per headgroup over 50 ns simulation time of a fully lipolyzed POPC bilayer membrane. Average values calculated are 0.81 ± 0.02 nm^2 at pH 9.0, 0.66 ± 0.01 nm^2 at pH 7.5, and 0.54 ± 0.01 nm^2 at pH 5.5.

0.01 nm^2 at pH 7.5, and 0.54 ± 0.01 nm^2 at pH 5.5, as presented in Fig. 2. For comparison, the simulation-based average area per lipid for the POPC lipid membrane is 0.68 nm^2 ± 0.01 nm^2 (T = 310 K) [36], which is close to the experimental value of 0.683 ± 0.015 nm^2 (T = 303 K) [53]. Interestingly, the lowest area per molecule at pH 5.5 is comparable to the area per lipid found in sphingomyelin bilayers above their main phase transition temperature [54,55], indicating a similar type of ordering in the bilayer.

The increase in the area per headgroup with increasing pH can be easily understood by considering the number of charged molecules in the systems. When the fraction of charged oleates increases with increasing pH, the repulsive interactions between oleate molecules also increases leading to a larger area per molecule. This idea and our results are also in agreement with Langmuir monolayer experiments [56], in which the area per molecule of phospholipid/cardiolipin (90:10) monolayer increased by 8.6% when the pH was increased from pH 4 to pH 8.

The suggested pH dependence of the equlibrium area per molecule may be important, if vesicles or lipid droplets are exposed to pH gradients after PLA_2 modification. Here we assume that vesicles or lipid droplets are initially spherical and stable before exposure to a pH gradient. In equlibrium both systems can be described using the Laplace law [57]

$$\Delta P = 2\frac{\gamma}{R} \quad (1)$$

where ΔP is the pressure difference between the inner and outer membrane, γ is the surface tension and R is the radius of the particle. According to this equation, the surface tension and pressure difference in a stable vesicle are zero without osmotic pressure. If such a vesicle is exposed to a pH gradient that changes the area per molecule, a tension and pressure difference will occur in the bilayer. A decrease in pH would result in decreased surface area, and induce positive surface tension and positive pressure. A vesicle can remove the induced tension by changing the amount of solvent inside the core, either directly through the lipid membrane or through membrane pores. If the lipolysis and pH gradient occur on only one side of the vesicle membrane, curvature frustration will occur in the bilayer due to the asymmetric change in the area. Such curvature frustration could be removed by lipid flip-flops or the absorption or desorption of lipids.

For a spherical lipid droplet of a given volume, decreasing the pH could also lead to an increased surface tension, since at low pH values, the FFAs are uncharged at the surface monolayer. Negatively charged FFAs are more hydrophilic than uncharged FFAs, and therefore they tend to lower the surface tension of an oil–water interface. Furthermore, the surface tension of a spherical particle can return to the original value if lipid molecules absorb on the surface or if the particle size decreases. However, when compared to the rapid fusion of membranes induced by increased surface tension, these two processes are likely to be too slow [58] to prevent membrane fusion. By applying this idea to our results, we suggest that increased surface tension at low pH might enhance the fusion of vesicles and lipid droplets.

3.2. Electron density profiles across bilayer

Information about the general structure of the bilayer along the normal was obtained by computing electron density profiles for the whole system, different molecular species, as well as P atoms from the MD trajectories of the three simulated pH systems. The simulation boxes were divided into 0.1 nm slices, and the number of electrons for each type of atom was given. The electron densities are shown in Fig. 3. The most obvious difference between the three simulated systems is the different overall membrane thickness; all of the profiles

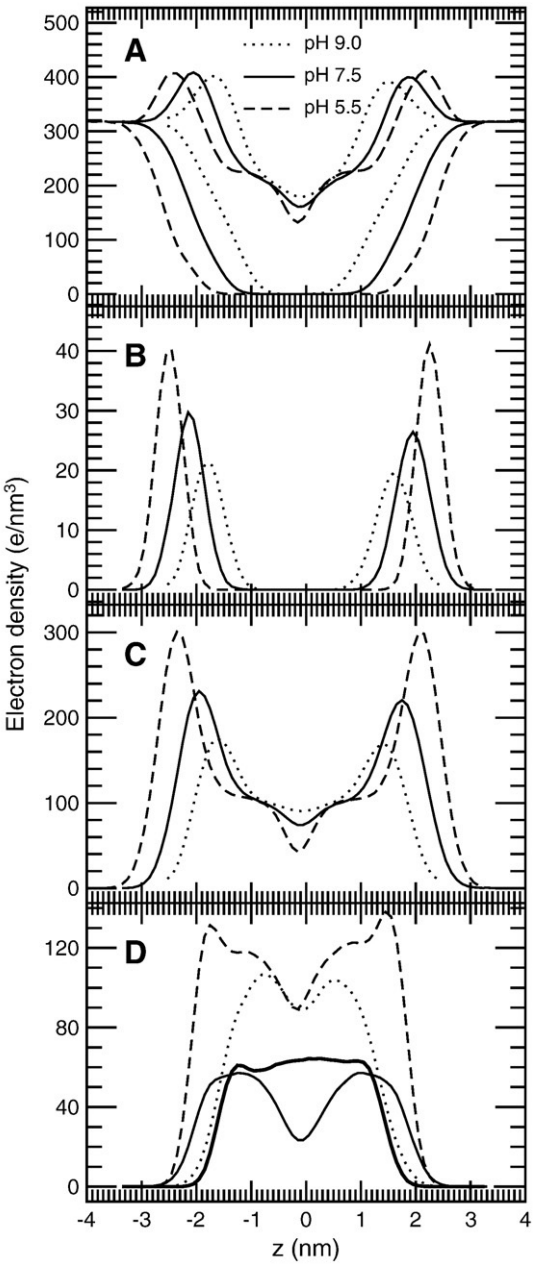

Fig. 3. Electron density profiles as functions of distance z from the bilayer center at pH 9.0 (dotted line), at pH 7.5 (solid line), and at pH 5.5 (dashed line). A. Total systems together with water layers. B. Head group phosphorus (P) atoms allowing the calculation of average P–P distance between opposite leaflets. C. LysoPC molecules. D. Oleic acid and oleate molecules.

are consistent with a thickening of the bilayer with decreasing pH value.

Fig. 3A shows the electron densities of the total systems together with the water slabs. The total electron density profiles have a maximum corresponding approximately to the location of the phosphate headgroups, and a minimum, a so-called methyl trough, in the bilayer center where the terminal methyl groups reside. When the pH decreases, the headgroup–headgroup distance increases, i.e., the bilayer becomes thicker, and the electron density in the bilayer center decreases. The penetration of water into the bilayer becomes more difficult with decreasing pH, which reflects both the thickening of the bilayer and the increasing densities in the headgroup regions.

In Fig. 3B the distance d_{PP} is calculated between the maxima of the phosphate electron density profiles, and it is the actual distance

between the electron-dense phosphate peaks. The results show that a decrease in pH increases the distance between headgroups in opposite leaflets. The obtained distance d_{PP} values are 3.4 nm, 4.1 nm, and 4.8 nm for pH 9.0, 7.5 and 5.5, respectively.

Fig. 3D shows the electron density profiles of the FFAs. At pH 7.5, the electron density profile of the oleic acid molecules has a plateau at the bilayer center, whereas the oleate molecules have lower density in the bilayer center and are pushed towards the water phase. They are therefore responsible for the trough seen in the total electron density profile.

Thinning of the bilayer with increasing pH is again in line with the increasing area per headgroup due to the increased repulsion between charged FFAs.

3.3. Chain structures

When simulating molecules with long carbon tails, it is of interest to describe their ordering with respect to the normal of the membrane. The deuterium order parameter has been determined as

$$S_{CD} = {}^{1}/_{2}\langle 3\cos^2\theta - 1\rangle \quad (2)$$

where θ is the angle between the bilayer normal (the z axis of the simulation box) and the C–H bond vector. The brackets denote averaging over all lipids and different time frames. The order parameter can vary between one (full order along the bilayer normal) and −one half (full order perpendicular to the bilayer normal). To calculate deuterium order parameters from Eq. (2), the positions of hydrogen atoms had to be included in the trajectories, which was performed by calculating the positions on the basis of the orientation of carbon chains and exploiting tetrahedral symmetry at given sites. A similar approach was used to study other lipid bilayers [36,54].

We computed the order parameters separately for both chains, *sn*-1 and *sn*-2. The ordering effect of decreasing pH is clearly visible; the order parameters grow significantly with decreasing pH. This is in agreement with the results for the area per headgroup; the order increases with decreasing area per headgroup. Of note, as the chains become more ordered at low pH, their order parameter values get closer to those of sphingomyelin bilayers [59].

Fig. 4 shows the S_{CD} profiles of lysoPC, oleate, and oleic acid at different pH values. The order parameter profiles of lysoPC decay at pH 7.5 and 9.0, whereas at pH 5.5, the order parameter profile shows merely a plateau for the beginnings and central parts of the chains, and a decay near the center of the bilayer (Fig. 4A). The order parameter profile for oleate is more ordered at pH 7.5 than at pH 9.0 (Fig. 4B). For oleic acid at pH 5.5 and at pH 7.5, the order parameter profiles show a plateau for the beginnings of the chains (carbons 2 to 7), and the characteristic drop in the double bond region (carbons 8 to 11) (Fig. 4C). The electron density profiles (Fig. 3) demonstrate that oleates reside closer to the bilayer surface than oleic acids, which may explain the increased order of the oleates. In general, the order parameters of the chain segments are larger near the surface [36]. For comparison, the order parameters of the fatty acid chains of the unhydrolyzed POPC bilayer are also shown in all Fig. 4 panels; at pH 7.5, the beginning of the palmitoyl chain of lysoPC and the free oleate chain are slightly more ordered as compared to the ones in the unhydrolysed POPC bilayer.

3.4. Lateral pressure profiles

We first discuss the physical theory from which the calculations of the lateral pressure profiles are derived. In a lipid bilayer, the surface energy between the hydrophobic and hydrophilic phases tends to minimize the area, such that in the equilibrium steric, electrostatic and dispersion interactions cancel the energy. This balance creates a non-uniform pressure distribution through the lipid bilayer, which is often described using the lateral pressure profile

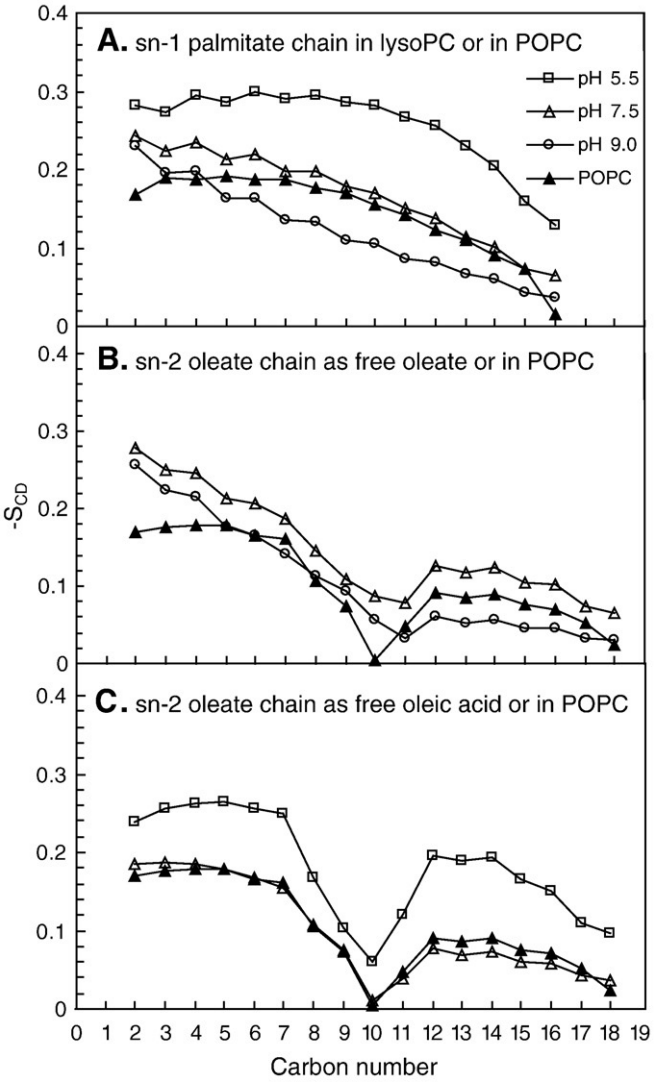

Fig. 4. SCD profiles of lysoPC (A), oleate (B), and oleic acid (C) in simulations mimicking the FFA composition at pH 9.0 (open circles), 7.5 (open tiangles), and 5.5 (open squares), as well as *sn*-1 and *sn*-2 chains of POPC bilayer (solid triangles).

$$p(z) = \frac{P_{xx}(z) + P_{yy}(z)}{2} - P_{zz}(z), \quad (3)$$

where the coordinate z is along the membrane normal and P is the pressure tensor [57,60–62]. The lateral pressure profile is connected to the elastic properties of bilayers and monolayers, and it has been suggested that it is related to membrane protein functionality [61,63,64]. Here, our primary interest is the effect of decreased pH on the lateral pressure profile of a lipolyzed phospholipid bilayer. In addition, we use the lateral pressure profiles as a tool to analyze the elastic properties of phospholipid bilayers.

The lateral pressure profile is related to the product of the bending modulus κ_m and the spontaneous curvature c_0^m through its first moment [57]

$$\kappa_m c_0^m = \int_0^h dz(z-\delta)p(z) \quad (4)$$

and to the Gaussian bending modulus $\bar{\kappa}_m$ through its second moment

$$\bar{\kappa}_m = -\int_0^h dz(z-\delta)^2 p(z), \quad (5)$$

where z is the normal coordinate of the layer and δ is the position of the neutral monolayer plane (see below). Here we define $z=0$ to be the center of the bilayer and h to be the monolayer thickness. The terms c_0^m,κ_m, and $\bar{\kappa}_m$ refer to monolayer properties. Thus, Eqs. (4) and (5) give elastic properties of a monolayer in a bilayer.

The above equations and the pressure profiles have been used in several previous studies for the analysis of elastic properties of monolayers [48,65,66]. The deficiency of the equations is that the location of the neutral plane δ is not defined. Therefore, in previous studies, two different pressure profile characteristics were used to identify δ: the minimum of the surface peak [66], and the first maximum corresponding to the chain region [67]. We chose δ to be the point midway between the positions of these features. To estimate the error, we repeated the calculation for both δ positions used previously. The parameters computed according to Eqs. (4) and (5) were done for both leaflets and then averaged.

The lateral pressure profiles were calculated for systems representing different pH values and are presented in Fig. 5. We see the well-recognized features of a lateral pressure profile in all of our systems: the negative peak in the interface between polar and nonpolar areas due to the surface energy, and positive contributions due to electrostatic, steric, and dispersion interactions in the headgroup and acyl chain regions [62]. With increasing pH we find systematic changes in the pressure profile: the negative peaks from opposite leaflets move closer to each other, indicating a decrease in the membrane thickness; and both the negative interfacial peak and the positive contributions from the acyl chain regions decrease in magnitude. The latter observation is especially interesting because it suggests that repulsive pressure is transferred from the acyl chain region to the headgroup region, thus introducing positive spontaneous curvature at increasing pH values.

To analyze this phenomenon more quantitatively, we used the relationship between spontaneous curvature and the lateral pressure profile, Eq. (4). We also calculated the Gaussian bending modulus using the second moment of the pressure profile, Eq. (5). The results are gathered in Table 2, and show that a decrease in pH indeed has an effect on the product of the bending modulus and spontaneous curvature $\kappa_m c_0^m$. However, the exact values of the bending modulus and spontaneous curvature are unknown. In principle, the bending modulus could be extracted from simulation data by using the undulation spectrum, but that would require a much larger simulation system size and length [68]. On the other hand, κ_m always has a positive value and we see that the sign of the product $\kappa_m c_0^m$ is changed when moving from pH 7.5 to pH 5.5. Hence, the sign of the spontaneous curvature has to change from positive to negative when shifting from pH 7.5 to pH 5.5. We also see a decrease in the product when shifting from pH 9 to pH 7.5, but the sign is unchanged, so this

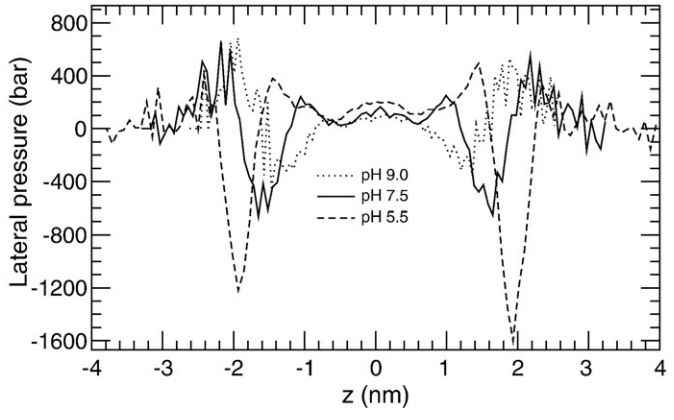

Fig. 5. Lateral pressure profiles across a fully lipolyzed POPC membrane at pH 9.0, (dotted line), at pH 7.5 (solid line), and at pH 5.5 (dashed line).

Table 2
Product of the bending modulus and the spontaneous curvature $\kappa_m c_0^m$ and the Gaussian bending modulus $\bar{\kappa}_m$. Values were calculated from the lateral pressure profiles and are given as mean ± error.

pH	$\kappa_m c_0^m \times 10^{-11}\frac{J}{m}$	$\bar{\kappa}_m \times 10^{-20}$J
9.0	3 ± 1	−3 ± 2
7.5	1 ± 1	−2.7 ± 2
5.5	−3 ± 1	−3 ± 2

difference could be produced by a change in κ_m. In general, the results lead to one important conclusion: in a membrane composed solely of lysoPC and FFA, spontaneous curvature decreases with decreasing pH, and the sign of the curvature shifts from positive at pH 7.5 to negative at pH 5.5.

Our results are in agreement with experimental studies, which suggest that low pH values in phosphatidic acid membranes promote the presence of the inverted hexagonal H_{II} phase, especially when divalent positive ions are present (Mg^{2+} or Ca^{2+}) [7–9]. This is logical, as with low pH values the headgroup charges are neutralized due to protonation, which leads to a decrease in repulsive interactions between headgroups and thus the effective headgroup size. The presence of positive ions further screens out negative charge repulsions between headgroups and transforms membrane curvature in the negative direction [7,69]. We also calculated the Gaussian bending modulus for the two opposing monolayer leaflets in our lipolyzed POPC bilayers, and the results are presented in Table 2. All values obtained are within the calculated error bars, thus we cannot see any pH effect on the Gaussian bending modulus.

Because the spontaneous curvature c_0^m and the Gaussian bending modulus $\bar{\kappa}_m$ appear to play a role in the stalk formation occurring during vesicle fusion process [4,5,70], the elastic properties of monolayers are of great theoretical and practical interest. Indeed, it has been concluded that (1) the negative spontaneous curvature of a monolayer c_0^m and (2) the low Gaussian bending modulus $\bar{\kappa}_m$ ease stalk formation, which, again, is a critical step towards membrane fusion [4,67]. Stalk formation would also be a plausible trigger for lipid droplet and lipoprotein particle fusion [71]; theoretical studies on fusion of emulsion particles suggest that a decrease in spontaneous curvature of surface monolayers promotes phase behaviour where the particles are fused [72–74]. We suggest that provided the low Gaussian bending modulus decreases the energy of stalk formation in vesicle fusion, the modulus would also facilitate the fusion of lipid droplets and liporotein particles.

By connecting the above ideas to the present results, we can argue that with decreasing pH the spontaneous curvature of a monolayer decreases, which may (1) enhance fusion events, and (2) decrease the phase transition temperature to the inverted phase. These predictions are in agreement with previous experimental studies where low pH was found to induce inverted phase formation when divalent positive ions were present (Mg^{2+} or Ca^{2+}) [7–9]. This picture is also in agreement with experimental findings that PA lipids, together with positive ions and low pH, enhance vesicle fusion [75–79].

On the other hand, in our simulated systems, comprised of lysoPCs and FFAs in the pH range 9.0–5.5, we did not find any correlation between the Gaussian bending modulus and pH. The behaviour of the Gaussian bending modulus is not very well known but it is believed to scale in the same way as the bending modulus [70]. Thus, for our system, we find the pH dependence of spontaneous curvature more significant than the pH dependence of elastic constants.

3.5. Conclusions

In this study, we aimed at revealing pH-induced changes in the properties of a fully lipolyzed POPC bilayer membrane, so mimicking exposure of a nanoregion of a cellular membrane to an acidic

environment, such as occurs inside in various subcellular compartments, notably the lysosomes. Importantly, the extracellular fluids of advanced atherosclerotic lesions and of large solid tumors are acidic [26,80]. Thus, the phospholipids of the plasma membranes of cells residing in such areas are also exposed to acidic pH. Finally, the secretory PLA_2 is able to modify lipoprotein particles in the extracellular fluid [81,82], and there is ample evidence suggesting that it plays a role in the development of atherosclerosis [83].

The major effects of pH are shown in Fig. 6 [84]. The most obvious pH effect found was that decreased pH was associated with decreased area per headgroup, which reflects decreased headgroup repulsions. This change, again, resulted in many structural effects in the membranes. Thus, at low pH, the lipid hydrocarbon chains were found to have larger orientational order parameter values, indicating a higher degree of order in the hydrocarbon chains along the bilayer normal. Also, as reflected in the electron density profiles across the membrane, membrane thickness was found to increase with decreasing pH. As membrane thickness is an important factor in determining the functional protein-dependent characteristics of a given membrane [3,85,86], even small changes in membrane thickness may have significant effects on the conformation of membrane proteins. Adding sodium chloride [87] or cholesterol, or increasing the fatty acid chain length, have all been shown to increase the bilayer thickness, whereas an increase in chain unsaturation or an increase in the strength of headgroup repulsions cause the bilayer to thin [88]. As predicted by the present simulations, variation of pH within the range 9.0–5.5 influences the thickness of a lipolyzed, but not an unlipolyzed, POPC bilayer.

Enzymatic modifications of various membrane lipid species are thought to be responsible for local changes in the spontaneous curvature of biological membranes [16]. These changes, again, are involved in membrane fission and fusion [2], and also affect various functions of the membrane proteins [3]. However, because the molecular shapes of certain lipolyzed lipids (e.g. lysophosphatidic acid) have a strong dependence on pH [7], certain lipids have more than one value for spontaneous curvature. This phenomenon is clearly observed in the present results, which suggest that the value of spontaneous curvature shifts in the negative direction with decreasing pH in a membrane formed solely of lysoPCs and FFAs. Hence, PLA_2 hydrolysis could create local membrane nanoareas formed of lysoPCs and FFAs in a bilayer separating two compartments that differ in pH. The monolayer leaflet facing the acidic compartment would have negative spontaneous curvature while the monolayer leaflet facing the alkalic compartment would have positive spontaneous curvature, thus creating a local membrane curvature required for membrane fission.

Our findings from bilayers can also be related to the properties of phospholipid monolayers covering intracellular lipid droplets [89] and extracellular lipoprotein particles or lipid droplets [90], as the properties of such surface monolayers resemble those of the outer bilayer leaflet [91]. The behaviour of these monolayers is involved in many physiologically important events. Thus, intracellular lipid droplets are considered to be dynamic organelles controlling lipid storage and efflux [92,93], and their surface lipid monolayer plays a pivotal role in controlling the docking of various regulatory proteins and enzymes. Any perturbation of the monolayer covering atherogenic lipoprotein particles, again, can trigger aggregation and fusion of the modified lipoprotein particles, so leading to lipid accumulation in atherosclerotic lesions [94]. Regarding the fusion process, it has been suggested that negative spontaneous curvature would ease up the stalk formation [4,11]. Our results show that, at acidic pH, a monolayer composed of lysoPC and oleic acid molecules has a net negative spontaneous curvature, which leads to a hypothesis that PLA_2 hydrolysis of lipid droplets or lipoprotein particles at acidic pH conditions may lead to their fusion.

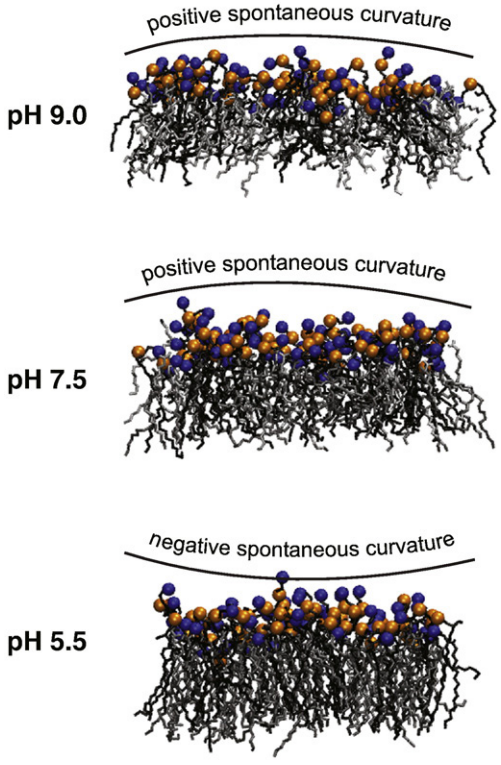

Fig. 6. Monolayer structures at the end of simulation at pH 9.0, 7.5, or 5.5. For clarity, water molecules and opposing monolayer leaflets are not shown. The acyl chains have been rendered with bonds (colors: lysoPC black, FFA grey), whereas headgroup phosphorus and nitrogen are rendered with VDW (colors: phosphorus orange, nitrogen blue). The lower the pH, the smaller the area per lipid, the more ordered the lipid hydrocarbon chains, and the thicker the membrane. Also, the value of spontaneous curvature shifts from positive to negative, as the value of pH reaches 5.5.

Acknowledgements

The Wihuri Research Institute is maintained by the Jenny and Antti Wihuri Foundation. We thank the Finnish IT Center for Science for computer resources. This work has been supported by the Academy of Finland 107368 (PTK) and the Nanoscience Graduate School (OHSO). We wish to thank Dr. Katariina Öörni for valuable discussions regarding the biochemistry of lipolysis in acidic pH environments, and Dr. Sarah Overduin for proofreading the manuscript.

References

[1] W. Dowhan, M. Bogdanov, Functional roles of lipids in membranes, in: D.E. Vance, J.E. Vance (Eds.), New Comprehensive Biochemistry, vol. 36, Biochemistry of Lipids, Lipoproteins and Membranes, Elsevier Science B.V, Amsterdam, 2002, pp. 1–35.
[2] K.N. Burger, Greasing membrane fusion and fission machineries, Traffic 1 (2000) 605–613.
[3] R. Phillips, T. Ursell, P. Wiggins, P. Sens, Emerging roles for lipids in shaping membrane-protein function, Nature 459 (2009) 379–385.
[4] L.V. Chernomordik, M.M. Kozlov, Mechanics of membrane fusion, Nat. Struct. Mol. Biol. 15 (2008) 675–683.
[5] L.V. Chernomordik, M.M. Kozlov, Protein–lipid interplay in fusion and fission of biological membranes, Annu. Rev. Biochem. 72 (2003) 175–207.
[6] E.E. Kooijman, V. Chupin, N.L. Fuller, M.M. Kozlov, K.B. de, K.N. Burger, P.R. Rand, Spontaneous curvature of phosphatidic acid and lysophosphatidic acid, Biochemistry 44 (2005) 2097–2102.
[7] E.E. Kooijman, V. Chupin, K.B. de, K.N. Burger, Modulation of membrane curvature by phosphatidic acid and lysophosphatidic acid, Traffic 4 (2003) 162–174.
[8] A.J. Verkleij, M.R. De, J. Leunissen-Bijvelt, K.B. de, Divalent cations and chlorpromazine can induce non-bilayer structures in phosphatidic acid-containing model membranes, Biochim. Biophys. Acta 684 (1982) 255–262.
[9] S.B. Farren, M.J. Hope, P.R. Cullis, Polymorphic phase preferences of phosphatidic acid: A ^{31}P and ^{2}H NMR study, Biochem. Biophys. Res. Commun. 111 (1983) 675–682.
[10] H.T. McMahon, J.L. Gallop, Membrane curvature and mechanisms of dynamic cell membrane remodelling, Nature 438 (2005) 590–596.

[11] P.K. Kinnunen, J.M. Holopainen, Mechanisms of initiation of membrane fusion: role of lipids, Biosci. Rep. 20 (2000) 465–482.
[12] S. Zellmer, G. Cevc, P. Risse, Temperature- and pH-controlled fusion between complex lipid membranes. Examples with the diacylphosphatidylcholine/fatty acid mixed liposomes, Biochim. Biophys. Acta 1196 (1994) 101–113.
[13] V. Knecht, S.J. Marrink, Molecular dynamics simulations of lipid vesicle fusion in atomic detail, Biophys. J. 92 (2007) 4254–4261.
[14] J.E. Burke, E.A. Dennis, Phospholipase A_2 biochemistry, Cardiovasc. Drugs Ther. 23 (2009) 49–59.
[15] M. Murakami, I. Kudo, Phospholipase A_2, J. Biochem. 131 (2002) 285–292.
[16] W.J. Brown, K. Chambers, A. Doody, Phospholipase A_2 (PLA_2) enzymes in membrane trafficking: mediators of membrane shape and function, Traffic 4 (2003) 214–221.
[17] O.G. Berg, M.H. Gelb, M.D. Tsai, M.K. Jain, Interfacial enzymology: the secreted phospholipase A_2-paradigm, Chem. Rev. 101 (2001) 2613–2654.
[18] P. de Figueiredo, D. Drecktrah, J.A. Katzenellenbogen, M. Strang, W.J. Brown, Evidence that phospholipase A_2 activity is required for Golgi complex and trans Golgi network membrane tubulation, Proc. Natl Acad. Sci. USA 95 (1998) 8642–8647.
[19] M. Rigoni, P. Caccin, S. Gschmeissner, G. Koster, A.D. Postle, O. Rossetto, G. Schiavo, C. Montecucco, Equivalent effects of snake PLA_2 neurotoxins and lysophospholipid-fatty acid mixtures, Science 310 (2005) 1678–1680.
[20] A. Gubern, M. Barcelo-Torns, J. Casas, D. Barneda, R. Masgrau, F. Picatoste, J. Balsinde, M.A. Balboa, E. Claro, Lipid droplet biogenesis induced by stress involves triacylglycerol synthesis that depends on group VIA phospholipase A_2, J. Biol Chem 284 (2009) 5697–5708.
[21] P. Boström, M. Rutberg, J. Ericsson, P. Holmdahl, L. Andersson, M.A. Frohman, J. Borén, S.O. Olofsson, Cytosolic lipid droplets increase in size by microtubule-dependent complex formation, Arterioscler. Thromb. Vasc. Biol. 25 (2005) 1945–1951.
[22] W. Yu, P.T. Bozza, D.M. Tzizik, J.P. Gray, J. Cassara, A.M. Dvorak, P.F. Weller, Co-compartmentalization of MAP kinases and cytosolic phospholipase A_2 at cytoplasmic arachidonate-rich lipid bodies, Am. J. Pathol. 152 (1998) 759–769.
[23] R.E. Wooten, M.C. Willingham, L.W. Daniel, C.C. Leslie, L.C. Rogers, S. Sergeant, J.T. O'Flaherty, Novel translocation responses of cytosolic phospholipase A_2 alpha fluorescent proteins, Biochim. Biophys. Acta 1783 (2008) 1544–1550.
[24] K. Lähdesmäki, R. Plihtari, P. Soininen, E. Hurt-Camejo, M. Ala-Korpela, K. Öörni, P.T. Kovanen, Phospholipase A_2-modified LDL particles retain the generated hydrolytic products and are more atherogenic at acidic pH, Atherosclerosis 207 (2009) 352–359.
[25] J.A. Shayman, A. Abe, M. Hiraoka, A turn in the road: how studies on the pharmacology of glucosylceramide synthase inhibitors led to the identification of a lysosomal phospholipase A_2 with ceramide transacylase activity, Glycoconj. J. 20 (2004) 25–32.
[26] M. Naghavi, R. John, S. Naguib, M.S. Siadaty, R. Grasu, K.C. Kurian, W.B. van Winkle, B. Soller, S. Litovsky, M. Madjid, J.T. Willerson, W. Casscells, pH Heterogeneity of human and rabbit atherosclerotic plaques; a new insight into detection of vulnerable plaque, Atherosclerosis 164 (2002) 27–35.
[27] M. Kimura-Matsumoto, Y. Ishikawa, K. Komiyama, T. Tsuruta, M. Murakami, S. Masuda, Y. Akasaka, K. Ito, S. Ishiguro, H. Morita, S. Sato, T. Ishii, Expression of secretory phospholipase A2s in human atherosclerosis development, Atherosclerosis 196 (2008) 81–91.
[28] E. Hurt-Camejo, G. Camejo, H. Peilot, K. Öörni, P. Kovanen, Phospholipase A_2 in vascular disease, Circ. Res. 89 (2001) 298–304.
[29] H.J.C. Berendsen, D. van der Spoel, R. van Drunen, Gromacs: a message-passing parallel molecular dynamics implementation. Comput. Phys. Commun. 91 (1995) 43–56.
[30] E. Lindahl, B. Hess, D. van der Spoel, GROMACS 3.0: a package for molecular simulation and trajectory analysis, J. Mol. Mod. 7 (2001) 306–317.
[31] D.P. Tieleman, H.J.C. Berendsen, Molecular dynamics simulations of a fully hydrated dipalmitoylphosphatidylcholine bilayer with different macroscopic boundary conditions and parameters, J. Chem. Phys. 105 (1996) 4871.
[32] O. Berger, O. Edholm, F. Jahnig, Molecular dynamics simulations of a fluid bilayer of dipalmitoylphosphatidylcholine at full hydration, constant pressure, and constant temperature, Biophys. J. 72 (1997) 2002–2013.
[33] S.W. Chiu, M. Clark, V. Balaji, S. Subramaniam, H.L. Scott, E. Jakobsson, Incorporation of surface tension into molecular dynamics simulation of an interface: a fluid phase lipid bilayer membrane, Biophys. J. 69 (1995) 1230–1245.
[34] W.F. van Gunsteren, P. Krüger, S.R. Billeter, A.E. Mark, A.A. Eising, W.R.P. Scott, Hüneberg P.H., and I.G. Tironi, Biomolecular Simulation: the GROMOS96 Manual and User Guide. Biomos, Groningen and Hochsuchulverlag AG, Germany and Er ETH Zürich, Zurich, Switzerland., 1996.
[35] D.P. Tieleman, H.J. Berendsen, A molecular dynamics study of the pores formed by Escherichia coli OmpF porin in a fully hydrated palmitoyloleoylphosphatidylcholine bilayer, Biophys. J. 74 (1998) 2786–2801.
[36] S. Ollila, M.T. Hyvönen, I. Vattulainen, Polyunsaturation in lipid membranes: dynamic properties and lateral pressure profiles, J. Phys. Chem B 111 (2007) 3139–3150.
[37] D.M. Small, D.J. Cabral, D.P. Cistola, J.S. Parks, J.A. Hamilton, The ionization behavior of fatty acids and bile acids in micelles and membranes, Hepatology 4 (1984) 77S–79S.
[38] B. Hess, H. Bekker, H.J.C. Berendsen, J.G.E.M. Fraaije, LINCS: a Linear Constraint Solver for molecular simulations, J. Comp. Chem. 18 (1997) 1463–1472.
[39] S. Miyamoto, P.A. Kollman, Settle: an analytical version of the SHAKE and RATTLE algorithm for rigid water models, J. Comp. Chem. 13 (1992) 952–962.
[40] U. Essman, L. Perela, M.L. Berkowitz, T. Darden, H. Lee, L.G. Pedersen, A smooth particle mesh Ewald method, J. Chem. Phys. 103 (1995) 8577–8592.
[41] M. Patra, M. Karttunen, M.T. Hyvönen, E. Falck, P. Lindqvist, I. Vattulainen, Molecular dynamics simulations of lipid bilayers: major artifacts due to truncating electrostatic interactions, Biophys. J. 84 (2003) 3636–3645.
[42] T. Rog, K. Murzyn, M. Pasenkiewicz-Gierula, Molecular dynamics simulations of charged and neutral lipid bilayers: treatment of electrostatic interactions, Acta Biochim. Pol. 50 (2003) 789–798.
[43] H.J.C. Berendsen, J.P.M. Postma, W.F. van Gunsteren, A. DiNola, J.R. Haak, Molecular dynamics with coupling to an axternal bath. J. Chem. Phys. 81 (1984) 3684–3690.
[44] S. Nosé, A molecular dynamics method for simulations in the canonical ensemble, Mol. Phys. 52 (1984) 255–268.
[45] W.G. Hoover, Canonical dynamics: equilibrium phase-space distributions, Physical Review A 31 (1985) 1695–1697.
[46] M. Parrinello, A. Rahman, Polymorphic transitions in single crystals: a new molecular dynamics method, J. Appl. Phys. 52 (1981) 7182–7190.
[47] S. Nosé, M.L. Klein, Constant pressure molecular dynamics for molecular systems, Mol. Phys. 50 (1983) 1055–1076.
[48] O.H.S. Ollila, T. Rog, M. Karttunen, I. Vattulainen, Role of sterol type on lateral pressure profiles of lipid membranes affecting membrane protein functionality: comparison between cholesterol, desmosterol, 7-dehydrocholesterol and ketosterol, J. Struct. Biol 159 (2007) 311–323.
[49] P.S. Niemelä, S. Ollila, M.T. Hyvönen, M. Karttunen, I. Vattulainen, Assessing the nature of lipid raft membranes, PLoS. Comput. Biol 3 (2007) e34.
[50] E. Terämä, O.H. Ollila, E. Salonen, A.C. Rowat, C. Trandum, P. Westh, M. Patra, M. Karttunen, I. Vattulainen, Influence of ethanol on lipid membranes: from lateral pressure profiles to dynamics and partitioning, J. Phys. Chem B 112 (2008) 4131–4139.
[51] O.H.S. Ollila and I. Vattulainen, Lateral pressure profiles in lipid membranes: dependence on molecular composition, in: Phillip Biggin, Mark Sansom (Eds.), Molecular Simulations and Biomembranes: From Biophysics to Function, Royal Society of Chemistry (in press).
[52] J.H. Irving, J.G. Kirkwood, The Statistical Mechanical Theory of Transport Processes. IV. The Equations of Hydrodynamics, J. Chem. Phys. 18 (1950) 817.
[53] N. Kucerka, S. Tristram-Nagle, J.F. Nagle, Structure of fully hydrated fluid phase lipid bilayers with monounsaturated chains, J. Membr. Biol 208 (2005) 193–202.
[54] P. Niemelä, M.T. Hyvönen, I. Vattulainen, Structure and dynamics of sphingomyelin bilayer: insight gained through systematic comparison to phosphatidylcholine, Biophys. J. 87 (2004) 2976–2989.
[55] P.R. Maulik, G.G. Shipley, X-ray diffraction and calorimetric study of N-lignoceryl sphingomyelin membranes, Biophys. J. 69 (1995) 1909–1916.
[56] N. Khalifat, N. Puff, S. Bonneau, J.B. Fournier, M.I. Angelova, Membrane deformation under local pH gradient: mimicking mitochondrial cristae dynamics, Biophys. J. 95 (2008) 4924–4933.
[57] S.A. Safran, Statistical Thermodynamics of Surfaces, Interfaces, and Membranes, Addison-Wesley, Reading, MA, 1994.
[58] J. Lyklema, Fundamentals of Interface and Colloid Science, vol. III: Liquid–fluid interfaces, Academic press, London, UK, 2000.
[59] P.S. Niemelä, M.T. Hyvönen, I. Vattulainen, Influence of chain length and unsaturation on sphingomyelin bilayers, Biophys. J. 90 (2006) 851–863.
[60] J.S. Rowlinson, B. Widom, Molecular Theory of Capillarity, Clarendon press, Oxford, 1982.
[61] D. Marsh, Lateral pressure in membranes, Biochim. Biophys. Acta 1286 (1996) 183–223.
[62] J.N. Israelachvili, Intermolecular and Surface Forces, Academic Press, London, 1985.
[63] S. Robert, Cantor, lateral pressures in cell membranes: a mechanism for modulation of protein function, The Journal of Physical Chemistry B 101 (1997) 1723–1725.
[64] M.F. Brown, Modulation of rhodopsin function by properties of the membrane bilayer, Chem. Phys. Lipids 73 (1994) 159–180.
[65] S.J. Marrink, H.J. Risselada, S. Yefimov, D.P. Tieleman, A.H. de Vries, The MARTINI force field: coarse grained model for biomolecular simulations, J. Phys. Chem B 111 (2007) 7812–7824.
[66] M. Orsi, D.Y. Haubertin, W.E. Sanderson, J.W. Essex, A quantitative coarse-grain model for lipid bilayers, J. Phys. Chem B 112 (2008) 802–815.
[67] R.H. Templer, B.J. Khoo, J.M. Seddon, Gaussian curvature modulus of an amphiphilic monolayer, Langmuir 14 (2009) 7427–7434.
[68] E. Lindahl, O. Edholm, Mesoscopic undulations and thickness fluctuations in lipid bilayers from molecular dynamics simulations, Biophys. J. 79 (2000) 426–433.
[69] E.R. May, D.I. Kopelevich, A. Narang, Coarse-grained molecular dynamics simulations of phase transitions in mixed lipid systems containing LPA, DOPA, and DOPE lipids, Biophys. J. 94 (2008) 878–890.
[70] D.P. Siegel, The Gaussian curvature elastic energy of intermediates in membrane fusion, Biophys. J. 95 (2008) 5200–5215.
[71] M.O. Pentikäinen, M.T. Hyvönen, K. Öörni, T. Hevonoja, A. Korhonen, E.M. Lehtonen-Smeds, M. Ala-Korpela, P.T. Kovanen, Altered phospholipid-apoB-100 interactions and generation of extra membrane material in proteolysis-induced fusion of LDL particles, J. Lipid Res. 42 (2001) 916–922.
[72] Edgar M. Blokhuis, Wiebke F.C. Sager, Vesicle adhesion and microemulsion droplet dimerization: small bending rigidity regime, J. Chem. Phys. 111 (1999) 7062.
[73] D.N. Petsev, Structure and film formation in charged emulsions and microemulsions, Physica A 250 (1998) 115–132.
[74] A. Kabalnov, H. Wennerström, Macroemulsion Stability, The Oriented Wedge Theory Revisited, 1996, pp. 276–292.
[75] S. Ichikawa, P. Walde, Phospholipase D-mediated aggregation, fusion, and precipitation of phospholipid vesicles, Langmuir 20 (2004) 941–949.

[76] R. Sundler, N. Duzgunes, D. Papahadjopoulos, Control of membrane fusion by phospholipid head groups. II. The role of phosphatidylethanolamine in mixtures with phosphatidate and phosphatidylinositol, Biochim. Biophys. Acta 649 (1981) 751–758.
[77] J.B. Park, Interaction of phospholipase D to vesicles induces membrane fusion, Experimental and Molecular Medicine 28 (1996) 141.
[78] M.A. Churchward, T. Rogasevskaia, D.M. Brandman, H. Khosravani, P. Nava, J.K. Atkinson, J.R. Coorssen, Specific lipids supply critical negative spontaneous curvature—an essential component of native Ca2+-triggered membrane fusion, Biophys. J. 94 (2008) 3976–3986.
[79] J.B. Park, T.H. Lee, H. Kim, Fusion of phospholipid vesicles induced by phospholipase D in the presence of calcium ion, Biochem. Int. 27 (1992) 417–422.
[80] P. Swietach, R.D. Vaughan-Jones, A.L. Harris, Regulation of tumor pH and the role of carbonic anhydrase 9, Cancer Metastasis Rev. 26 (2007) 299–310.
[81] N.R. Webb, Secretory phospholipase A_2 enzymes in atherogenesis, Curr. Opin. Lipidol. 16 (2005) 341–344.
[82] M.A. Boström, B.B. Boyanovsky, C.T. Jordan, M.P. Wadsworth, D.J. Taatjes, F.C. de Beer, N.R. Webb, Group V Secretory Phospholipase A2 Promotes Atherosclerosis. Evidence From Genetically Altered Mice, Arterioscler. Thromb. Vasc. Biol. 27 (2007) 600–606.
[83] K. Öörni, P.T. Kovanen, Lipoprotein modification by secretory phospholipase A_2 enzymes contributes to the initiation and progression of atherosclerosis, Curr. Opin. Lipidol. 20 (2009) 421–427.
[84] W. Humphrey, A. Dalke, K. Schulten, VMD—Visual Molecular Dynamics, J. Molec. Graphics 14 (1996) 33–38.
[85] O.S. Andersen, R.E. Koeppe, Bilayer thickness and membrane protein function: an energetic perspective, Annu. Rev. Biophys. Biomol. Struct. 36 (2007) 107–130.
[86] J.A. Lundbaek, O.S. Andersen, Spring constants for channel-induced lipid bilayer deformations. Estimates using gramicidin channels, Biophys. J. 76 (1999) 889–895.
[87] R.A. Böckmann, A. Hac, T. Heimburg, H. Grubmüller, Effect of sodium chloride on a lipid bilayer, Biophys. J. 85 (2003) 1647–1655.
[88] R.S. Cantor, Lipid composition and the lateral pressure profile in bilayers, Biophys. J. 76 (1999) 2625–2639.
[89] K. Tauchi-Sato, S. Ozeki, T. Houjou, R. Taguchi, T. Fujimoto, The surface of lipid droplets is a phospholipid monolayer with a unique Fatty Acid composition, J. Biol. Chem. 277 (2002) 44507–44512.
[90] R. Prassl, P. Laggner, Molecular structure of low density lipoprotein: current status and future challenges, Eur. Biophys. J. 38 (2009) 145–158.
[91] A. Koivuniemi, M. Heikelä, P.T. Kovanen, I. Vattulainen, M.T. Hyvönen, Atomistic simulations of phosphatidylcholines and cholesteryl esters in high-density lipoprotein-sized lipid droplet and trilayer: clues to cholesteryl ester transport and storage, Biophys. J. 96 (2009) 4099–4108.
[92] J.M. Goodman, The gregarious lipid droplet, J. Biol Chem 283 (2008) 28005–28009.
[93] S.O. Olofsson, P. Boström, L. Andersson, M. Rutberg, J. Perman, J. Borén, Lipid droplets as dynamic organelles connecting storage and efflux of lipids, Biochim. Biophys. Acta 1791 (2009) 448–458.
[94] K. Öörni, M.O. Pentikäinen, M. Ala-Korpela, P.T. Kovanen, Aggregation, fusion, and vesicle formation of modified low density lipoprotein particles: molecular mechanisms and effects on matrix interactions, J. Lipid Res. 41 (2000) 1703–1714.